Energy Impact of Different Penetrations of Connected and Automated Vehicles: A Preliminary Assessment

Jackeline Rios-Torres and Andreas A. Malikopoulos
Energy and Transportation Science Division
Oak Ridge National Laboratory
Oak Ridge, TN 37831 USA
riostorresj@ornl.gov, andreas@ornl.gov

ABSTRACT
Previous research reported in the literature has shown the benefits of traffic coordination to alleviate congestion, and reduce fuel consumption and emissions. However, there are still many remaining challenges that need to be addressed before a massive deployment of fully automated vehicles. This paper aims to investigate the energy impacts of different penetration rates of connected and automated vehicles (CAVs) and their interaction with human-driven vehicles. We develop a simulation framework for mixed traffic (CAVs interacting with human-driven vehicles) in merging roadways and analyze the energy impact of different penetration rates of CAVs on the energy consumption. The Gipps car following model is used along with heuristic controls to represent the driver decisions in a merging roadways traffic scenario. Using different penetration rates of CAVs, the simulation results indicated that for low penetration rates, the fuel consumption benefits are significant but the total travel time increases. The benefits in travel time are noticeable for higher penetration rates of CAVs.

CCS Concepts
Computing methodologies ~ Simulation support systems.

Keywords
Connected and automated vehicles; cooperative merging control; merging highways; vehicle coordination; car following; mixed traffic simulation.

1. INTRODUCTION
Merging roadways are one of the primary sources of traffic congestion [1], [2]. The required coordination of maneuvers that are required in a limited period of time to safely merge onto the main road traffic, makes merging roadways one of the main sources of driver discomfort and frustration. The stress experienced by drivers when merging may encourage a more aggressive driving behavior and further slow the traffic flow, increasing the fuel consumption [3]. In 2014, traffic congestion resulted in people expending 6.9 billion of extra hours on the road and an estimated cost of $160 billion in extra fuel [4].

Connected and automated vehicles (CAVs) can provide shorter gaps between vehicles and faster responses while improving highway capacity. Given the recent technological developments, several research efforts have considered approaches to achieve safe and efficient coordination of merging maneuvers with the intention to avoid severe stop-and-go driving. Research efforts using either centralized or decentralized approaches have focused on coordinating CAVs in specific traffic scenarios [5]. The overarching goal of vehicle coordination is to yield a smooth traffic flow aimed at avoiding stop-and-go driving. One of the very early efforts in this direction was proposed in 1969 by Athans [6]. Assuming a given merging sequence, Athans formulated the merging problem as a linear optimal regulator to control a single string of vehicles, with the aim of minimizing the speed errors that will affect the desired headway between each consecutive pair of vehicles. Later, Schmidt and Posch [7] proposed a two-layer control scheme based on heuristic rules that were derived from observations of the non-linear system dynamics behavior. Similar to the approach proposed in [6], Awal *et al.* [8] developed an algorithm that starts by computing the optimal merging sequence to achieve reduced merging times for a group of vehicles that are closer to the merging point.

More recently, the problem of coordinating vehicles that are wirelessly connected to each other at merging roads was addressed in [9], [10]. A closed-form solution was developed aimed at optimizing the acceleration profile online of each vehicle in terms of fuel economy while avoiding collision with other vehicles at the merging zone. The proposed solution was validated through simulation and it was shown that coordination of connected vehicles can reduce fuel consumption at merging roads by up to 50%.

Although previous research reported in the literature has shown the benefits of autonomous traffic coordination control to alleviate traffic congestion and reduce fuel consumption and emissions, many challenges have to be addressed before a massive deployment of fully automated vehicles. It is expected, however, that CAVs will penetrate in the market slowly and interact with non-autonomous vehicles.

This paper aims to investigate the energy impacts of different penetration rates of CAVs and their interaction with human-driven vehicles. The contribution of this paper is the development of a simulation framework for mixed traffic (CAVs interacting with human-driven vehicles) in a merging roadway scenario and, the analysis of the energy impact of different penetration rates of

IWCTS'16, October 31-November 03 2016, Burlingame, CA, USA
© 2016 ACM. ISBN 978-1-4503-4577-4/16/10…$15.00
DOI: http://dx.doi.org/10.1145/3003965.3003969

CAVs on fuel consumption. We assume the CAVs are controlled by the control algorithm reported in [9], [10]. A baseline scenario is developed in which "human-driven" vehicles attempt to merge into a main road using the Gipps car following model to represent the driver decisions (speed at each instant of time).

2. METHODOLOGY

We address the merging scenario shown in Figure 1, where a secondary one-lane road merges onto a main one-lane road. Typically, the vehicles on the secondary road yield to the vehicles on the main road and wait until a safe opportunity is perceived to merge onto the main road. We assume that a portion of the vehicles on the roads are CAVs while the remaining are human-driven vehicles (non-CAVs) that will attempt to merge by using only observations of their surroundings. The CAVs are controlled using the optimization framework and control algorithms reported in [9], [10]. The human-driven vehicles (non-CAVs) follow heuristic rules and the Gipps car following model [11] to represent the driver behavior and decisions regarding the speed. Then, the two control frameworks are combined to evaluate the energy impacts produced by different penetration rates of CAVs. In the following subsections we describe the two control approaches.

2.1 Modeling approach for human-driven vehicles

We consider the merging roadways of Figure 1 and use the Gipps car following model [12] to represent the driver decisions. The Gipps model adjust the driver behavior with the aim to keep a safe following distance from the leader vehicle. There are two conditions to guarantee a collision-free trip 1) $\tau_{gap} \geq 3\tau / 2$, and 2) $u_{f,\min} \geq \hat{u}_{l,\min}$, where τ_{gap} is the time gap with respect to the leader, τ represents the "apparent" driver reaction time and it is the simulation sample time, $u_{f,\min}$ is the highest allowed braking and $\hat{u}_{l,\min}$ the follower estimation of the highest braking the leader can achieve [11], [13], [14]. In the Gipps model, the speed v of the follower vehicle is computed as

$$v_f(t+\tau) = \min\{v_{f,acc}(t+\tau), v_{f,dec}(t+\tau)\}\ , \qquad (1)$$

where $v_{f,acc}$ is the speed when the vehicle is not constrained by the traffic flow and $v_{f,dec}$ is the speed when the vehicle is constrained by a leader in front and they are calculated as

$$v_{f,acc}(t+\tau) = v_f(t) + 2.5 u_{f,\max}\tau\left(1 - \frac{v_f(t)}{v_{f,\max}}\right)\sqrt{0.025 + \frac{v_f(t)}{v_{f,\max}}} \qquad (2)$$

$$v_{f,dec}(t+\tau) = u_{f,\min}\tau + \sqrt{u_{f,\min}^2\tau^2 - u_{f,\min}\left[\begin{array}{c} 2(p_l(t) - p_f(t) - (L_{veh} + fd)) \\ -v_f(t)\tau - \frac{v_f(t)}{\hat{u}_{l,\min}} \end{array}\right]}, \qquad (3)$$

were f, l identify the follower and the leader respectively, p is the vehicle position, v is the vehicle speed, $v_{f,\max}$ is the maximum desired speed, $u_{f,\max}$ is the maximum desired acceleration, $u_{f,\min}$ is the highest allowed braking value, $\hat{u}_{l,\min}$ is the follower's estimation of the leader highest braking value, L_{veh} is the vehicle length and, fd is the desired following distance. In our work, the desired following distance was chosen to keep the 2-second rule and the Gipps following model is applied to compute the speed attained for all the human-driven vehicles (non-CAVs). The 2-second rule establishes that the time gap between two consecutive vehicles should be at least two seconds to safely stop in case the vehicle in front suddenly brakes.

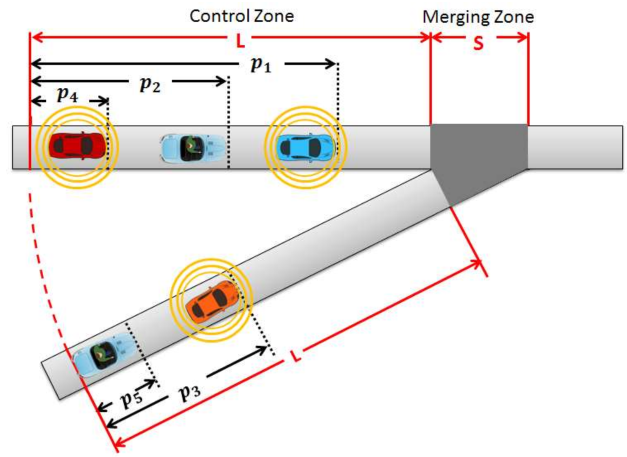

Figure 1. Merging roads with connected and automated vehicles interacting with human-driven vehicles.

The details of the algorithm are included in Table 1.

A vehicle traveling on the main road will consider its preceding vehicle on the road as its leader and will follow the speed dictated by the Gipps model until it reaches the merging zone, i.e., $p_f = P_{Merging}$. Once in the merging zone, the vehicle will evaluate whether there is a vehicle merging in front, in such case, it will start considering the merging vehicle as its new leader. Similarly, a vehicle traveling on the secondary road will consider its preceding vehicle on the road as its leader until its position reaches a distance γ from the merging zone (this section of the road of length γ before the merging zone will be identified as the pre-merging zone for non-CAVs). Once there, the "driver" starts evaluating the merging conditions and looks for the closest safe gap to merge by choosing a new potential leader and a new potential follower (p_{f-1}) in the main road. If the estimated time gap with the new potential follower is less than 1.5 s, the vehicle will start decelerating to be able to stop and avoid lateral collision in the merging zone. The "driver" will then wait until the next available gap to evaluate the merging conditions again. Once the vehicle merge, it will continue following the speed dictated by the Gipps car following model to try to keep a safe distance from its new leader on the main road.

2.2 Optimization framework to model CAVs behavior

We consider the merging roadways of Figure 1 where the CAVs are coordinated by using the optimization framework that will be briefly described next. Further details of the approach can be found in [9], [10]. The region of potential lateral collision of the vehicles is called merging zone and has a length S. There is also a control zone and a centralized controller that can control the vehicles traveling inside the control zone. The distance from the entry of the control zone until the entry of the merging zone is L.

Table 1. Merging algorithm for non-CAVs

```
Algorithm 1: Modeling Non-CAVs
Inputs
P_Merging = 400 m % Starting position of the merging zone
v_des = 13.41 m/s % Drivers desired speed
γ = 30 m % Distance to merging zone at which vehicles on secondary road will start
checking for a safe gap to merge into the main road
% v_{f-1}, p_{f-1} are the speed and position of the potential new follower on the main
road
Outputs: v_f, u_f, p_f

if vehicle is traveling on main road
    If vehicle is the first entering the control zone
        Accelerate to reach v_des
    else
        if p_f < P_Merging
            Use Gipps model to compute v_f, u_f, p_f such that a safe
            distance is kept with respect to the leader in the same road
        else
            Use Gipps model to compute v_f, u_f, p_f such that a safe
            distance is kept with respect to the closest vehicle in front
            (leader on the same road or a vehicle merging from the
            secondary road)
        end if
    end if
else
    If vehicle is the first approaching the merging zone
        Accelerate to reach v_des
    else
        if p_f > P_Merging − γ
            If p_f − p_{f-1} < 1.5 v_{f-1}
                Use Gipps model to compute v_f, u_f, p_f such that a
                safe distance is kept with respect to the new leader in
                the main road
            else
                Start decelerating to stop before reaching the merging
                zone and wait until the next available gap to evaluate
                for safe conditions to merge
            end if
        else
            Use Gipps model to compute v_f, u_f, p_f such that a safe
            distance is kept with respect to the leader in the same road
        end if
    end if
end if
```

We consider an increasing number of automated vehicles $N(t) \in \mathbb{N}$, where $t \in \mathbb{R}$ is the time, entering the control zone. When a vehicle reaches the control zone at some instant t the controller assigns a unique identity $i = N(t)+1$ that is an integer corresponding to the location of the CAV in a first-in-first-out (FIFO) queue for the control zone. If two or more vehicles enter the control zone at the same time, then the controller selects randomly their position in the queue. We consider that each vehicle is governed by a second order dynamics

$$\begin{aligned} \dot{p}_i &= v_i(t) \\ \dot{v}_i &= u_i(t) \end{aligned} \tag{4}$$

where $p_i(t) \in \mathcal{P}_i$, $v_i(t) \in \mathcal{V}_i$, and $u_i(t) \in \mathcal{U}_i$ denote the position, speed and acceleration/deceleration (control input) of each vehicle i. The sets $\mathcal{P}_i$, $\mathcal{V}_i$ and $\mathcal{U}_i$, $i \in \mathcal{N}_i(t)$, are complete and totally bounded subsets of $\mathbb{R}$. The state space $\mathcal{X}_i$ for each vehicle i is closed with respect to the induced topology on $\mathcal{P}_i \times \mathcal{V}_i$ and thus, it is compact.

2.2.1 Optimization Problem Formulation

We seek to address the problem of coordinating online an increasing number of automated vehicles on two merging roadways. The objective is to derive an analytical solution that yields the optimal control input at any time in terms of fuel consumption. For the latter, we use the polynomial metamodel proposed in [15] that yields vehicle fuel consumption as a function of the speed, v and control input, u.

To ensure that the control input and vehicle speed are within a given admissible range, the following constraints are imposed.

$$\begin{aligned} &u_{\min} \le u_i(t) \le u_{\max}, \text{ and} \\ &0 \le v_{\min} \le v_i(t) \le v_{\max}, \quad \forall t \in [t_i^0, t_i^f] \end{aligned} \tag{5}$$

where $u_{\min}$, $u_{\max}$ are the minimum deceleration and maximum acceleration respectively, and $v_{\min}$, $v_{\max}$ are the minimum and maximum speed limits respectively, t_i^0 is the time that vehicle i enters the control zone, and t_i^f is the time that vehicle i exits the merging zone.

To ensure the absence of rear-end collision of two consecutive vehicles traveling on the same lane, the position of the preceding vehicle should be greater than, or equal to the position of the following vehicle plus a predefined safe distance δ. The following definition refer to the case when the queue $\mathcal{N}(t)$ contains more than one vehicle.

Definition 2.1: For each vehicle i, we define the control interval R_i as

$$\begin{aligned} R_i \triangleq \{&u_i(t) \in [u_{\min}, u_{\max}] \mid p_i(t) \le p_k(t) - \delta, \\ &v_i(t) \in [v_{\min}, v_{\max}], \forall i \in \mathcal{N}(t), |\mathcal{N}(t)| > 1, \forall t \in [t_i^0, t_i^f]\}, \end{aligned} \tag{6}$$

where vehicle k is immediately ahead of i on the same road.

Definition 2.2: For each vehicle i, we define the set Γ_i as the set of all positions along the lane where a lateral collision is possible, namely

$$\begin{aligned} \Gamma_i \triangleq \{&p_i(t) \mid p_i(t) \in [L, L+S], \forall i \in \mathcal{N}(t), \\ &\mathcal{N}(t) > 1, \forall t \in [t_i^0, t_i^f]. \end{aligned} \tag{7}$$

To avoid lateral collision for any two vehicles i and j on different roads, the following constraint must hold

$$\Gamma_i \cap \Gamma_j = \varnothing, \forall t \in [t_i^0, t_i^f]. \tag{8}$$

The above constraint implies that only one vehicle, at a time, can be crossing the merging zone.

When a vehicle enters a control zone, it receives a unique identity i from the centralized controller. Recall that $\mathcal{N}(t) = \{1, \ldots, N(t)\}$ is the FIFO queue of vehicles in the control zone. A vehicle index $i \in \mathcal{N}(t)$ also indicates which vehicle is closer to the merging zone, i.e., for any $i, k \in \mathcal{N}(t)$ with $i < k$ then $p_i < p_k$.

Definition 3.1: Each vehicle $i \in \mathcal{N}(t)$ belongs to at least one of the following two subsets: 1) $\mathcal{L}_i(t)$ contains all vehicles traveling on the same road with i, and 2) $\mathcal{C}_i(t)$ contains all vehicles traveling on different roads from i.

The time t_i^f that the vehicle i exits the merging zone is based on imposing constraints aimed at avoiding congestion in the sense of maintaining vehicle speeds above a certain value. There are two cases to consider:

1) If vehicle $i-1$ belongs to $\mathcal{L}_i(t)$, then both $i-1$ and i should have the *minimal safe distance* allowable, denoted by δ, by the time vehicle $i-1$ enters the merging zone, i.e.,

$$t_i^f = t_{i-1}^f + \frac{\delta}{v_i(t_i^f)}, \tag{9}$$

where $v_i(t_i^f) = v_i(t_i^0)$ as we designate the vehicles to exit the merging zone with the same speed they had when they entered the control zone.

2) If vehicle $i-1$ belongs to $\mathcal{C}_i(t)$, we constrain the merging zone to contain only one vehicle so as to avoid a lateral collision. Therefore, vehicle i is allowed to enter the merging zone only when vehicle $i-1$ exits the merging zone, where t_i^m is the time that the vehicle i enters the merging zone, i.e.,

$$t_i^f = t_{i-1}^f + \frac{S}{v_i(t_i^f)}, \tag{10}$$

where $v_i(t_i^f) = v_i(t_i^0)$. Note that this recursive relationship over vehicles in a control zone queue satisfies both the rear-end and lateral collision avoidance constraints. We can then solve an optimization problem for each vehicle in the queue separately

$$\min_{u_i} \frac{1}{2}\int_{t_i^0}^{t_i^f} u_i^2 \tag{11}$$

Subject to: (2), (4) $\forall i \in \mathcal{N}(t)$.

2.2.2 Hamiltonian Analysis

For the analytical solution and online implementation of the problem (11), we apply Hamiltonian analysis [16]. To simplify the analysis, we consider the unconstrained problem and thus the optimal solution would not provide limits for the state and control. The constrained problem formulation is discussed in [17]. From (11) and the state equations (4), the Hamiltonian function can be formulated for each vehicle $i \in \mathcal{N}(t)$ as follows

$$H_i(t,x(t),u(t)) = L_i(t,x(t),u(t)) + \lambda^T \cdot f_i(t,x(t),u(t)), \tag{12}$$

Thus

$$H_i(t,x(t),u(t)) = \frac{1}{2}u_i^2 + \lambda_i^p \cdot v_i + \lambda_i^v \cdot u_i, \tag{13}$$

where λ_i^p and λ_i^v are the co-state components.

The Hamiltonian allows finding the optimal control input, speed and position for each vehicle as a function of time, namely

$$u_i^*(t) = a_i t + b_i, \tag{14}$$

$$v_i^*(t) = \frac{1}{2}a_i t^2 + b_i t + c_i, \tag{15}$$

$$p_i^*(t) = \frac{1}{6}a_i t^3 + \frac{1}{2}b_i t^2 + c_i t + d_i, \tag{16}$$

where c_i and d_i are constants of integration. To derive online the optimal control for each vehicle i, we need to update the integration constants at each time t. Equations (15) and (16), along with the initial and final conditions defined above, can be used to form a system of four equations of the form $\mathbf{T}_i\mathbf{b}_i = \mathbf{q}_i$, namely

$$\begin{bmatrix} \frac{1}{6}t^3 & \frac{1}{2}t^2 & t & 1 \\ \frac{1}{2}t^2 & t & 1 & 0 \\ \frac{1}{6}(t_i^f)^3 & \frac{1}{2}(t_i^f)^2 & t_i^f & 1 \\ \frac{1}{2}(t_i^f)^2 & t_i^f & t_i^f & 0 \end{bmatrix} \cdot \begin{bmatrix} a_i \\ b_i \\ c_i \\ d_i \end{bmatrix} = \begin{bmatrix} p_i(t) \\ v_i(t) \\ p_i(t_i^f) \\ d_i(t_i^f) \end{bmatrix}, \tag{17}$$

Thus (14) can be written as

$$u_i^*(t, p_i(t), v_i(t)) = a_i(t, p_i(t), v_i(t))t + b_i(t, p_i(t), v_i(t)). \tag{18}$$

Since (17) can be computed online, the controller can yield the optimal control online for each vehicle i, with feedback indirectly provided through the re-calculation of the vector $\mathbf{b}_i(t, p_i(t), v_i(t))$ in (17).

3. SIMULATION RESULTS

We simulated the scenario described in previous sections in Matlab assuming the control zone has a length $L = 400m$ and the merging zone a length of $S = 30m$. We assume that each non-CAV attempts to reach and maintain a desired speed $v_{des} = 13.41$ m/s while following the 2 s rule to maintain a safe distance from the leading vehicle and will use a pre-merging zone with length γ to evaluate the merging conditions and decide whether to merge or decelerate and wait for the next safe opportunity to merge. We also assume the CAVs attempt to reach and maintain a desired speed $v_{des} = 13.41$ m/s before entering the merging zone and after they leave the merging zone. When a CAV reaches the control zone the centralized controller designates its acceleration/deceleration until the vehicle exits the merging zone.

We considered two case studies: 1) 10 vehicles, all assumed to be non-CAVs and, 2) 30 vehicles attempting to merge in mixed traffic conditions, i.e., CAVs and non-CAVs. For the second case study, we simulated different penetration rates of CAVs on the road and compared the results with the baseline scenario in which all the 30 vehicles are assumed to be non-CAVs. To quantify the benefits in fuel consumption, we used the model in [15].

3.1.1 Case Study 1: 10 non-CAVs

We applied the heuristic control framework to 10 non-CAVs, 5 on each road. The purpose of this scenario is to confirm that the non-CAVs are able to safely cross the merging zone, i.e., no crashes occur.

The position trajectories in Figure **2** show that vehicles are able to cross the merging zone without collisions.

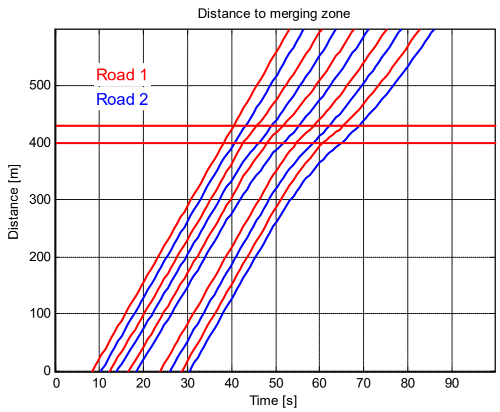

Figure 2. Position trajectories for the 30 vehicles on case study 1.

Once the vehicles reach the desired speed value, they have to start adjusting their speeds to keep a safe distance from their leading vehicles (Figure **3**). As expected, the variations in speed become more significant as the vehicles start getting closer to the merging zone.

3.1.2 Case Study 2: 30 vehicles in mixed traffic conditions

To assess the energy impacts of different penetration levels of CAVs on the traffic network, we combined the model approach for non-CAVs with the coordination framework for CAVs. Then, we simulated the merging scenario for 30 vehicles, 15 on each road, by assuming five different penetration rates of CAVs, i.e., 0% (baseline), 30%, 50%, 70%, and 100%. For each case, the CAVs were chosen randomly. We used the baseline scenario to assess the energy impacts of having a mix of CAVs and non-CAVs in the merging roads.

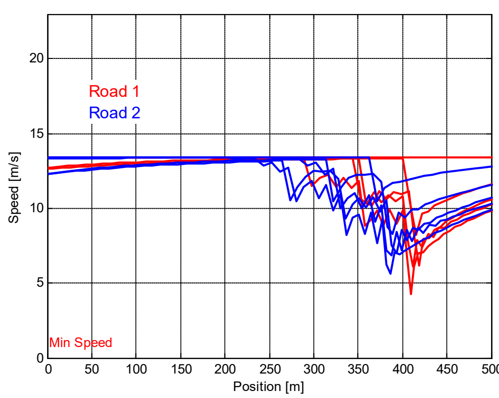

Figure 3. Speed profiles for the 10 vehicles in case study 1.

The speed profiles for the 0% penetration rate (baseline) show how the variations in speed become more significant as the vehicles approach the merging zone (Figure **4**). Congestion becomes unavoidable right before the merging zone, as some vehicles on the secondary road have to come to a full stop and wait until there is a safe gap to merge. When 50% of the vehicles are CAVs (Figure **5**), the variations in speed are more disperse along the control zone and some congestion occurs inside the first 200 m of the control zone. This "early" congestion is due to the CAVs attempting to adjust their speeds in advance to meet their safety constraints and the non-CAVs trying to keep a safe distance from their leaders on the respective roads. Note that to be able to meet the safety constraints some vehicles have to reach speeds above the desired value. When 100% of the vehicles are CAVs, the vehicles start adjusting their speed as soon as they reach the control zone to be able to meet the safety constraints (Figure **6**). This early planning allows to avoid congestion and to get a higher average speed.

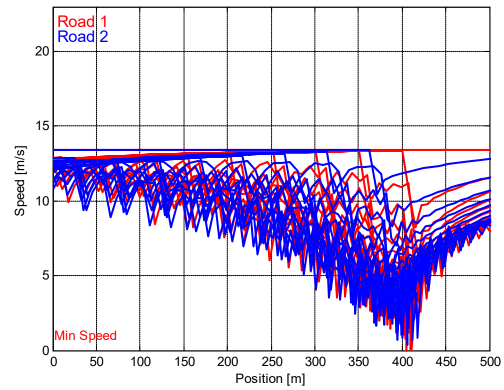

Figure 4. Speed profiles for the 30 vehicles in case study 2 with 0% CAVs penetration rate.

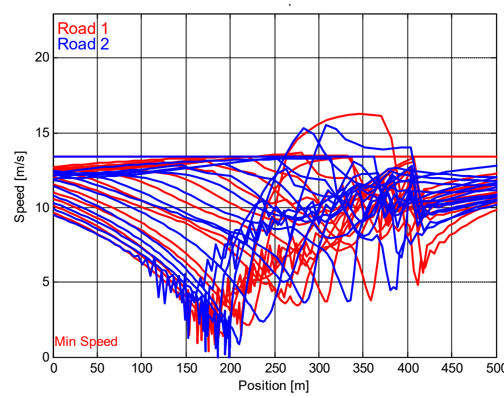

Figure 5. Speed profiles for the 30 vehicles in case study 2 with 50% CAVs penetration rate.

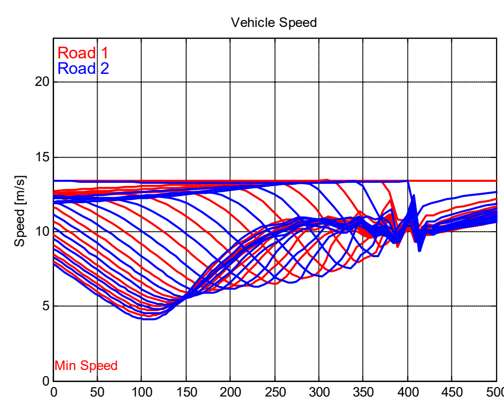

Figure 6. Speed profiles for the 30 vehicles in case study 2 with 100% CAVs penetration rate.

The fuel consumption results in Figure **7** suggest that even a penetration rate of 30% CAVs can have significant benefits in fuel consumption reduction (41%). However, as the penetration rate of CAVs increases, the rate of percentage benefits attenuates due to the variations is speed and the increased speed required in some cases to be able to meet the constraints. The highest benefit percentage is reached when all the vehicles are CAVs. In this last case, i.e, 100% penetration, the results are consistent with those reported in [9], [10], with benefits of about 50% in fuel consumption reduction.

The total travel time show instead an increment of about 1% when 30% of the vehicles attempting to merge are CAVs. The benefits in travel time appear when 70% of the vehicles are CAVs (about 2% reduction) and the maximum benefit of 5.43% is reached when all the vehicles are CAVs due to the increased average speed.

4. CONCLUSIONS

In this paper we developed a simulation framework to analyze the implications that different penetration rates of CAVs and their interaction with human-driven vehicles can have on energy consumption. The optimization framework proposed in [9], [10] was used to simulate the dynamics of CAVs that are optimally coordinated and a heuristic control approach based on the use of the Gipps car following model, was developed to model the dynamics of human-driven vehicles. Using different penetration rates of CAVs, the simulation results indicated that for low penetration rates, the fuel consumption benefits are significant but the total travel time increases.

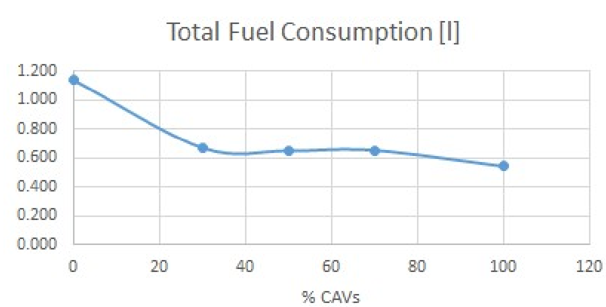

Figure 7. Total fuel consumption results for different penetration rates of CAVs.

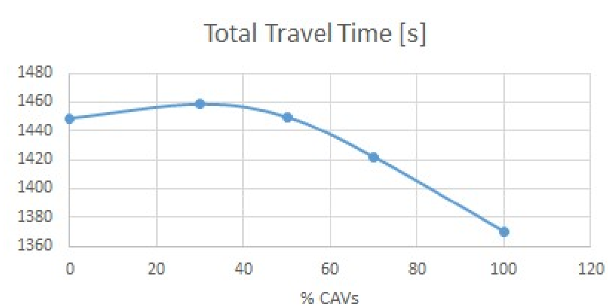

Figure 8. Total travel time for different penetration rates of CAVs.

5. ACKNOWLEDGEMENTS

This research was supported by DOE's SMART Mobility Initiative. This support is gratefully acknowledged.

6. REFERENCES

[1] R. Margiotta and D. Snyder, "An agency guide on how to establish localized congestion mitigation programs," 2011.

[2] A. A. Malikopoulos and J. P. Aguilar, "An Optimization Framework for Driver Feedback Systems," *IEEE Trans. Intell. Transp. Syst.*, vol. 14, no. 2, pp. 955–964, 2013.

[3] J. Sun, J. Ouyang, and J. Yang, "Modeling and Analysis of Merging Behavior at Expressway On-Ramp Bottlenecks," *Transp. Res. Rec. J. Transp. Res. Board*, vol. 2421, 2014.

[4] D. Schrank, B. Eisele, T. Lomax, and J. Bak, ""2015 Urban Mobility Scorecard, Texas A&M Transportation Institute 2015," 2015.

[5] J. Rios-Torres and A. A. Malikopoulos, "A Survey on Coordination of Connected and Automated Vehicles at Intersections and Merging at Highway On-Ramps," *IEEE Trans. Intell. Transp. Syst.*, p. (Forthcoming), 2016.

[6] M. Athans, "A unified approach to the vehicle-merging problem," *Transp. Res.*, vol. 3, no. 1, pp. 123–133, 1969.

[7] G. Schmidt and B. Posch, "A two-layer control scheme for merging of automated vehicles," *22nd IEEE Conf. Decis. Control*, pp. 495–500, 1983.

[8] T. Awal, L. Kulik, and K. Ramamohanrao, "Optimal traffic merging strategy for communication- and sensor-enabled vehicles," *Intell. Transp. Syst. - (ITSC), 2013 16th Int. IEEE Conf.*, pp. 1468–1474, 2013.

[9] J. Rios-Torres, A. A. Malikopoulos, and P. Pisu, "Online Optimal Control of Connected Vehicles for Efficient Traffic Flow at Merging Roads," *2015 IEEE 18th Int. Conf. Intell. Transp. Syst.*, 2015.

[10] J. Rios-Torres and A. A. Malikopoulos, "Automated and Cooperative Vehicle Merging at Highway On-Ramps," *IEEE Trans. Intell. Transp. Syst.*, p. (To appear), 2016.

[11] S. Panwai and H. Dia, "Comparative evaluation of microscopic car-following behavior," *IEEE Trans. Intell. Transp. Syst.*, vol. 6, no. 3, pp. 314–325, 2005.

[12] P. G. Gipps, "A behavioural car-following model for computer simulation," *Transp. Res. Part B Methodol.*, vol. 15, no. 2, pp. 105–111, Apr. 1981.

[13] L. Vasconcelos, L. Neto, S. Santos, A. B. Silva, and Á. Seco, "Calibration of the Gipps Car-following Model Using Trajectory Data," *Transp. Res. Procedia*, vol. 3, pp. 952–961, 2014.

[14] B. Ciuffo, V. Punzo, and M. Montanino, "Thirty Years of Gipps' Car-Following Model," *Transp. Res. Rec. J. Transp. Res. Board*, vol. 2315, pp. 89–99, Dec. 2012.

[15] M. A. S. Kamal, M. Mukai, J. Murata, and T. Kawabe, "Model Predictive Control of Vehicles on Urban Roads for Improved Fuel Economy," *IEEE Trans. Control Syst. Technol.*, vol. 21, no. 3, pp. 831–841, 2013.

[16] L. S. Pontryagin, *L.S. Pontryagin: Mathematical Theory of Optimal Processes*. CRC Press; English ed edition, 1987.

[17] M. Papageorgiou, M. Leibold, and M. Buss, *Optimierung: Statische, dynamische, stochastische Verfahren für die Anwendung*. Springer, 2012.